Microchimica Acta (2018) 185: 70
https://doi.org/10.1007/s00604-017-2613-5

ORIGINAL PAPER

Electrochemical quercetin sensor based on a nanocomposite consisting of magnetized reduced graphene oxide, silver nanoparticles and a molecularly imprinted polymer on a screen-printed electrode

Zufu Yao[1] · Xin Yang[2,3] · Xiaobo Liu[2] · Yaqi Yang[2] · Yangjian Hu[2] · Zijian Zhao[3]

Received: 8 September 2017 / Accepted: 6 December 2017 / Published online: 20 December 2017

Abstract

An electrochemical quercetin (QR) sensor is described that is based on the use of magnetic reduced graphene oxide (MrGO) incorporated into a molecularly imprinted polymer (MIP) on the surface of a screen-printed electrode (SPE). The MrGO consists of reduced graphene oxide (rGO), magnetite (Fe_3O_4) and silver nanoparticles (Ag). The analyte (QR) is electrostatically adsorbed on the surface of the MrGO. Finally, the MIP was deposited via in-situ polymerization. The composite was characterized by X-ray diffraction, Fourier transform infrared spectroscopy and Vibrating sample magnetometry. The morphologies and electrochemical properties of different electrodes were characterized by Field emission scanning electron microscopy, Electrochemical impedance spectroscopy and differential pulse voltammetry. Under optimal conditions, the modified electrode has a linear response in the 20 nM to 250 μM QR concentration range. The limit of detection is 13 nM (at an S/N ratio of 3). The electrode is selective, stable, regenerable and reliable. It was applied to the determination of QR in spiked pharmaceutical samples and gave satisfactory results.

Keywords Hybrid nanomaterial · Polymerization · Magnetite · XRD · FTIR · VSM · Nafion · Disposable sensor · FE-SEM · EIS · DPV

Introduction

Quercetin (QR) is one of typical natural flavonoids and has several biological activities. Developing analytical technologies and instruments to monitor this species is significant in clinics and pharmaceutics [1, 2]. Selective and sensitive determination of QR can be accomplished by high-performance liquid chromatography [3], chemiluminescence [4], capillary electrophoresis [5] and spectrophotometry [6]. However, those technologies and instruments are high cost inherently. Moreover, complicated pretreatments for samples are included. Worse still, expertise in handling the equipments is required and the operating process is time-consuming.

Several phenolic hydroxy groups exist in the QR molecular and can be oxidized on the electrode surface due to their electro-activities. Hence, electrochemical methods have been drawn considerable interest and used to detect QR successfully attributed to their portability, sensitivity, cheap and time-saving [7, 8]. Different electrochemical sensors have been fabricated to detect QR using various kinds of modifications. Ezhil Vilian reported gold nanoparticles (Au)-porous aromatic

Electronic supplementary material The online version of this article (https://doi.org/10.1007/s00604-017-2613-5) contains supplementary material, which is available to authorized users.

✉ Xin Yang
01yangxin@163.com

✉ Zijian Zhao
zjzhao72@163.com

[1] Hunan Provincial Key Laboratory of Dong Medicine, Hunan University of Medicine, Huaihua 418000, People's Republic of China

[2] Hunan Engineering Laboratory for Preparation Technology of Polyvinyl Alcohol Fiber Material, College of Chemistry and Materials Engineering, Huaihua University, Huaihua 418000, People's Republic of China

[3] Key Laboratory of Research and Utilization of Ethnomedicinal Plant Resources of Hunan Province, College of Biological and Food Engineering, Huaihua University, Huaihua 418000, People's Republic of China

framework (PAF-6) to modify glassy carbon electrode (GCE) for detecting QR [9]. QR was electrochemically determined using a platinum (Pt)-polydopamine (PDA) coated silica particles (SiO_2) modified GCE by Manokaran [10]. Li fabricated a simple and sensitive electrochemical sensor based on (graphene quantum dot)/Au nanocomposite modified GCE and utilized for the determination of QR [11].

However, some factors limit the electrochemical detection of QR under physiological conditions. One is the interferences from other flavonoids and ascorbic acid (AA) as their oxidation potential overlaps with that of QR at bare electrode. The other is that the concentration of QR is too low to detect in real pharmaceutical samples. To improve the measuring sensitivity and selectivity, an effective approach is to modify the electrode with conductive and selective materials.

Molecularly imprinted polymer (MIP) possesses binding sites complementary in shapes and sizes to recognize target molecules. It also represents chemical (physical) stability, low cost, easy preparation and resistance of harsh environmental condition compare with natural biological receptors, which is considered as an ideal artificial recognition material to improve the measuring selectivity [12–14]. Various MIPs modified electrodes have been widely used in determining of QR [15], propylparaben [16], glutathione [17], brucine [18], etc. based on these favorable properties of MIP. However, MIPs are organic materials and the use of them alone usually suffers from several drawbacks. For instance, slow mass transfer, poor binding kinetics and low binding capacity. Therefore, challenges still exist in fabricating an electrochemical sensor using MIP modified electrode.

Earlier studies revealed that the use of MIP combines with conductive nanomaterials can overcome the above difficulties. MIP combines to various conductive nanomaterials have been recommended to enlarge the electrochemical signal, such as reduced graphene oxide (rGO), silver nanoparticle (Ag) and magnetite (Fe_3O_4) [19–21]. Zeng introduced the free radical polymerization and prepared a novel composite consisting of rGO and MIP, using it as a recognition element to construct the 4-nitrophenol electrochemical sensor [19]. Li reported a novel salbutamol electrochemical sensing platform based on MIP incorporated with Ag-N-rGO [20]. Zhang fabricated an advanced amaranth magnetic molecularly imprinted electrochemical sensor (MIES) based on Fe_3O_4-rGO doped MIP membrane using magnetic field directed self-assembly [21]. Based on these advantages, we reasonably expect that the magnetic reduced graphene oxide (MrGO) consisting of rGO/Fe_3O_4- Ag combine MIP hybrid composite can provide good electrochemical sensitivity and selectivity for the determination of QR.

This study aims to fabricate a novel electrochemical sensor using MrGO-MIP composite to modify screen-printed electrode (SPE) for the determination of QR. Attributing to the synergistic effects originating from the combination of particles, the modified electrode (SPE | MrGO-MIP) exhibits improved sensitivity and selectivity. The modified electrode's surface can be renewed quickly via an external magnetic field. Finally, the electrochemical sensor is employed to detect QR in medicinal tablets with good accuracies and recoveries.

Experimental

Reagents and apparatus

Graphite, $AgNO_3$, $Fe(NO_3)_3{\cdot}9H_2O$, quercetin (QR), nafion solution, ethylene glycol dimethacrylate (EGDMA), acrylamide (AM), 2,2′-azobisisobutyronitrile (AIBN) and all other solvents and reagents with analytical reagent grade were obtained from sinopharm medicine holding co., ltd (http://www.sinoreagent.com/). The stock solutions of 0.1 M Na_2HPO_4 and 0.1 M NaH_2PO_4 were mixed with different proportion to prepare 0.1 M phosphate buffer (PB) at various pH values. Doubly distilled water (18.2 MΩ·cm) was used throughout. The Pule'an QR medicinal tablets were obtained nearby Hunan University of Medicine (20170412).

The Rigaku Ultima IV X-ray powder diffractometer (XRD, http://www.rigaku.com/en) and Shimadzu IR prestige-21 spectrometer were employed to record the crystallization degrees and fourier transform infrared spectroscopy (FTIR, http://www.shimadzu.com.cn/) spectra of the composite. The morphologies of various electrodes and quantitative analysis of the elements present in the composite were performed on the Zeiss Sigma HD field emission scanning electron microscope (FE-SEM, http://www.zeiss.com.cn/corporate/zh_cn/home. html) equipped with an Oxford instruments X-Max^N energy-dispersive X-ray spectrometer (EDS, http://www.oxford-instruments.cn/). The magnetic measurement was executed on the Lakeshore-736 vibrating sample magnetometer (VSM, http://www.lakeshore.com/ products/Vibrating-Sample-Magnetometer/Pages/Model-Landing.aspx).The DropSens corporation unmodified or modified screen-printed electrode (SPE) connected to the CHI 660D electrochemical workstation (Chenhua Instruments, http://www.chinstruments.com/) was used to perform the electrochemical measurements. The SPE was integrated with a carbon working electrode, an Ag/AgCl reference electrode and a carbon auxiliary electrode (http://www.dropsens.com/en/ home.html).

Synthesis of MrGO

The graphene oxide (GO) was synthesized from graphite with a modified Hummers method and cut into pieces and ground into powder for further use [22]. In a typical procedure [23], 4 mmol of $Fe(NO_3)_3{\cdot}9H_2O$ and 100.0 mg of GO were dispersed in 60 mL of ethyleneglycol followed by adding of

1.2 mmol $AgNO_3$ and 45 mmol NaAc. The mixture formed a clear solution after ultrasonicated for 90 min. The resulted suspension was subsequent transferred into a Teflon-lined stainless steel autoclave. The sealed autoclave was put into a furnace, heated to 200 °C and maintained for 2.0 h, then taken out and cooled in the air. Finally, the black precipitates were collected with magnetically and thoroughly rinsed by absolute ethanol and doubly distilled water and dried at 50 °C for 24 h.

Synthesis of MrGO-MIP

QR, AIBN, EGDMA and AM were acted as template molecules, initiator, cross- linking agent and functional monomer in the polymerization reaction [24, 25]. Briefly, 100 mg of dried MrGO was dispersed in 50 mL of organic mixture solvent ($V_{acetonitrile}$:V_{DMF} = 3:1) by ultrasonication for about 30 min. Then, 0.2 mmol QR was dispersed into the mixture solvent with ultrasonic treatment for 15 min. Finally, 0.8 mmol AM, 20.0 mg AIBN and 4.0 mmol EGDMA were added into the mixture under stirring and purged with N_2. The reaction was heated to 60 °C and maintained for 24 h. The MIP was dried, ground into powders and treated in a ultrasonic cleaner with a organic mixture solvent ($V_{methanol}$:$V_{acetic\ acid}$ = 9:1) for 1.0 h to remove the QR template, repeating the ultrasonic treatment five times. Finally, washing the MIP for 5 times by methanol to remove acetic acid residual and dried at 80 °C overnight. The procedures for MrGO-MIP preparation are described in Fig. 1a. Without adding the QR template molecule, the blank non-imprinted polymer (MrGO-NIP) was prepared using the same polymerization procedures.

Preparation of the modified electrode

20.0 mg of MrGO-MIP composite was dispersed in 4.0 mL of *wt.* 0.5% nafion solution to obtain a homogeneous suspension under vigorous ultrasonication. 10.0 μL of the suspension was deposited onto the working electrode and got dried under the infrared lamp (labeled as SPE│MrGO-MIP). For comparison, 10.0 μL of 5.0 mg·mL^{-1} MrGO and MrGO-NIP solutions were deposited onto other SPEs to fabricate the MrGO and MrGO-NIP modified SPE, respectively (labeled as SPE│MrGO and SPE│ MrGO-NIP).

Analytical procedures

The SPE│MrGO-MIP electrode was inserted into a beaker containing 2.0 mL of pH = 7.0 PB and purged N_2 for 10 min. Subsequently, various concentrations of QR standard solutions were addition into PB successively. The electrochemical performances of different electrodes and possible reduction mechanism of QR were investigated by cyclic voltammetry (CV) and differential pulse voltammetry (DPV). The CV measurements was carried out from −0.2 V to +0.8 V with a scan rate (v) of 0.1 V·s^{-1}. In DPV measurements, the scan was performed from −0.2 V to +0.5 V at a v of 100 mV·s^{-1} with the accumulation time and accumulation potential were 600 s and +0.05 V. The electrode's schematic diagram with possible reduction mechanism for QR is shown in Fig. 1b. The QR medicinal tablets after pretreatment were used as the real samples and followed the procedures recommended as above described. To identify the reliability of the method, the standard addition method was operated.

Results and discussion

Choice of materials

rGO is a widely-used graphene nanomaterial. Up to now, rGO-based materials have been emerged as one of novel nanomaterials in fabricating QR electrochemical sensor [26, 27]. Ag have many active sites as well as large electrochemically active surface area toward the electrochemical reaction of QR [28]. Thus, resulting in a high-performance amperometric response of QR molecules detection. The interference from other substances to QR determination can avoid by modifying the electrode surface with MIP film. Moreover, the Fe_3O_4 in the composite displays ferromagnetic behavior and can be rapidly magnetic separation with an external magnetic field. We reasonably expect that rGO, Ag and Fe_3O_4 in combination with MIP film can provide promising electrochemical activities for the electrochemical detection of QR.

Characterization of the MrGO-MIP composite

As shown in Fig. S1a, the characteristic graphite peak (2θ = 26°) disappears after oxidation and is replaced by a well-defined peak at 2θ = 10.8° corresponding to GO. The diffraction peaks relate to both Fe_3O_4 and Ag can be observed obviously in MrGO (Fig. S1b). Six characteristic peaks of Fe_3O_4 [2θ = 30.1° (220), 35.5° (311), 43.3° (400), 53.4° (422), 57.2° (511) and 62.5° (440)] are observed, which are in accordance with the face-centered cubic structure for the cubic phase Fe_3O_4 in the standard XRD data (JCPDS No.19–0629) [29]. Four peaks locate at 2θ = 77.7°, 64.6°, 44.4° and 38.2° indicate the (311), (220), (200) and (111) crystalline planes of Ag [23], respectively. No diffraction peaks arising from GO can be detected except the peaks assigned to Fe_3O_4 and Ag, which indicates that GO is reduced into rGO effectively. In MrGO-MIP (Fig. S1c) and MrGO-NIP (Fig. S1d) composites, no peaks relate to impurities are found.

The FTIR spectrum of GO displays -OH (3400 cm^{-1}), aromatic C=C (1620 cm^{-1}), carboxyl C-O (1410 cm^{-1}), alkoxy (1060 cm^{-1}), epoxy C-O (1230 cm^{-1}), and C=O (1730 cm^{-1}) in Fig. S2a [30]. However, as MrGO (Fig. S2b), the skeletal vibration related to the graphene (1620 cm^{-1}) is remained

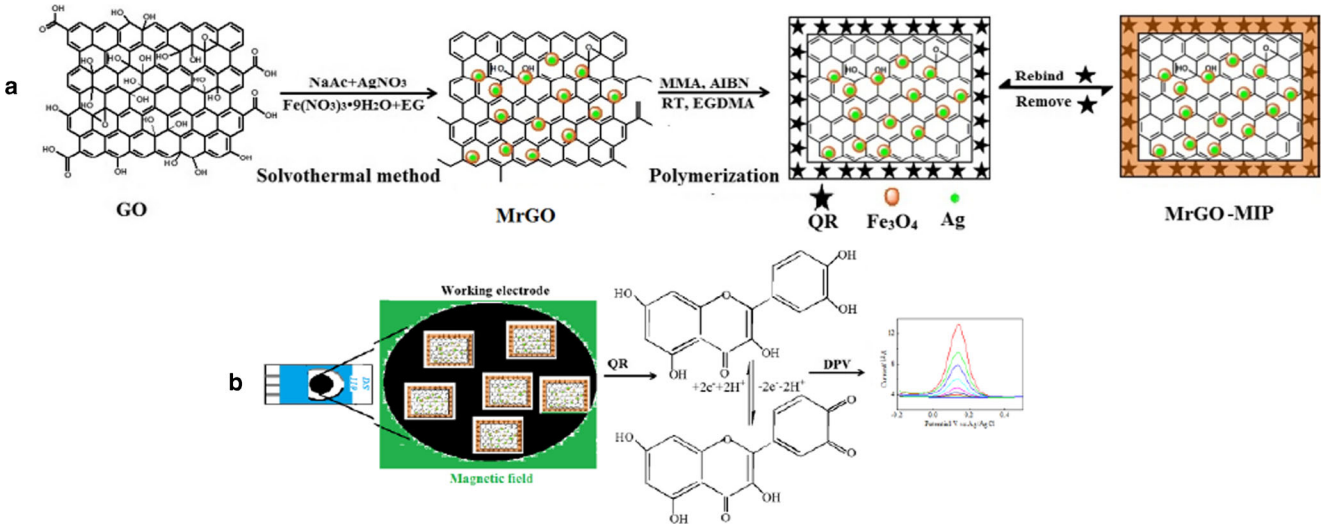

Fig. 1 Schematic illustration of the syntheses of MrGO-MIP composite (**a**) and the diagram of the electrode with possible reduction mechanism of QR (**b**)

although most oxygen-containing groups decreases or disappears, which indicates the presence of rGO [31]. The absorbance band at 588 cm^{-1} ascribes to Fe^{2+}-O^{2-} vibration and is consistent with the reported FTIR spectra for spinel Fe_3O_4 [32]. In MrGO-MIP spectrum (Fig. S2c), some absorption peaks range from 1000 cm^{-1} to 2000 cm^{-1} appear, which are attributed to the organic groups introduced from RT, AM and EDGMA in the MIP. Most characteristic absorption peaks of organic groups can be still found in the spectrum of MrGO-NIP (Fig. S2d).

The magnetic property of MrGO-MIP sample at room temperature is recorded by VSM using an applied field of −5000 Oe to 5000 Oe. The magnetic hysteresis loop shown in Fig. S3 indicates the ferromagnetic behavior of the composite. Due to the existence of Ag, rGO and MIP, the saturation magnetization of MrGO-MIP composite (52.1 $emu \cdot g^{-1}$) is lower than that of Fe_3O_4 (92 $emu \cdot g^{-1}$) [33]. The MrGO-MIP composite displaying ferromagnetic behavior and can be rapidly magnetic separation with an external magnetic field (about 90 s), which is critical to apply it in magnetic electrochemical sensors.

Characteristics of different electrodes

The flakes of graphite appear on the SPE (Fig. 2a) [34]. Massive MrGO nanoparticles seem to agglomerate via magnetic dipole-directed interaction (Fig. 2b). The total size of MrGO nanoparticle is about 25 nm. The EDS spectrum of MrGO is shown in Fig. 2e. The detectable elements include Ag, Fe, C and O. The C mainly comes from rGO. The O comes from the residual oxygen-containing functional groups of MIP and rGO. The detected Ag peak at nearby 3.1 keV is attributed to the Ag in the composite. Both the rGO and Ag can enhance the conductive property. No other impurity elements can be detected in the EDS analysis. There is great difference in the morphologies between the surfaces of SPE│MrGO-MIP (Fig. 2c) and SPE│MrGO-NIP electrodes (Fig. 2d). The MrGO-MIP membrane is rough while the MrGO-NIP membrane is homogeneous and smooth. The roughness of imprinted membrane on the SPE│MrGO -MIP electrode is beneficial for enhancing the response sensitivity and improving the rebinding efficiency of the sensor.

Electrochemical performances of various electrodes

The interfacial properties of various electrodes are studied with electrochemical impedance spectroscopy (EIS) (Fig. 3). The results are fitted to the Nyquist plots and the diameter of the semicircle part corresponds to the charge transfer resistance (Rct). The EIS of SPE shows a negligible Rct value with a very small semicircle diameter (Fig. 3a), implying that the characteristic of a diffusional limiting step of the $[Fe(CN)_6]^{3-/4-}$ electrochemical process [22, 30]. The Rct of SPE│MrGO electrode (Fig. 3b) increases a little, which is attributed to that the nafion used to fix nanomaterials can block the diffusion of $[Fe(CN)_6]^{3-/4-}$ although MrGO is highly electrical conductive. After SPE modified with the MrGO-MIP before removing of the template, the Rct increases remarkably (Fig. 3c), revealing that the MIP is immobilized on the surface successfully. The nonconductive MIP on the electrode's surface forms the barrier and blocks the exchange of electron between the electrode and solution [35]. The Rct decreases after the template removed (Fig. 3d), revealing that the template is removed successfully as well as the cavities formed which accelerates the electron exchanges. The Rct locates between MIP before and after removing of the QR when immobilized with MrGO-NIP in the same method (Fig. 3e). The reason may be due to that

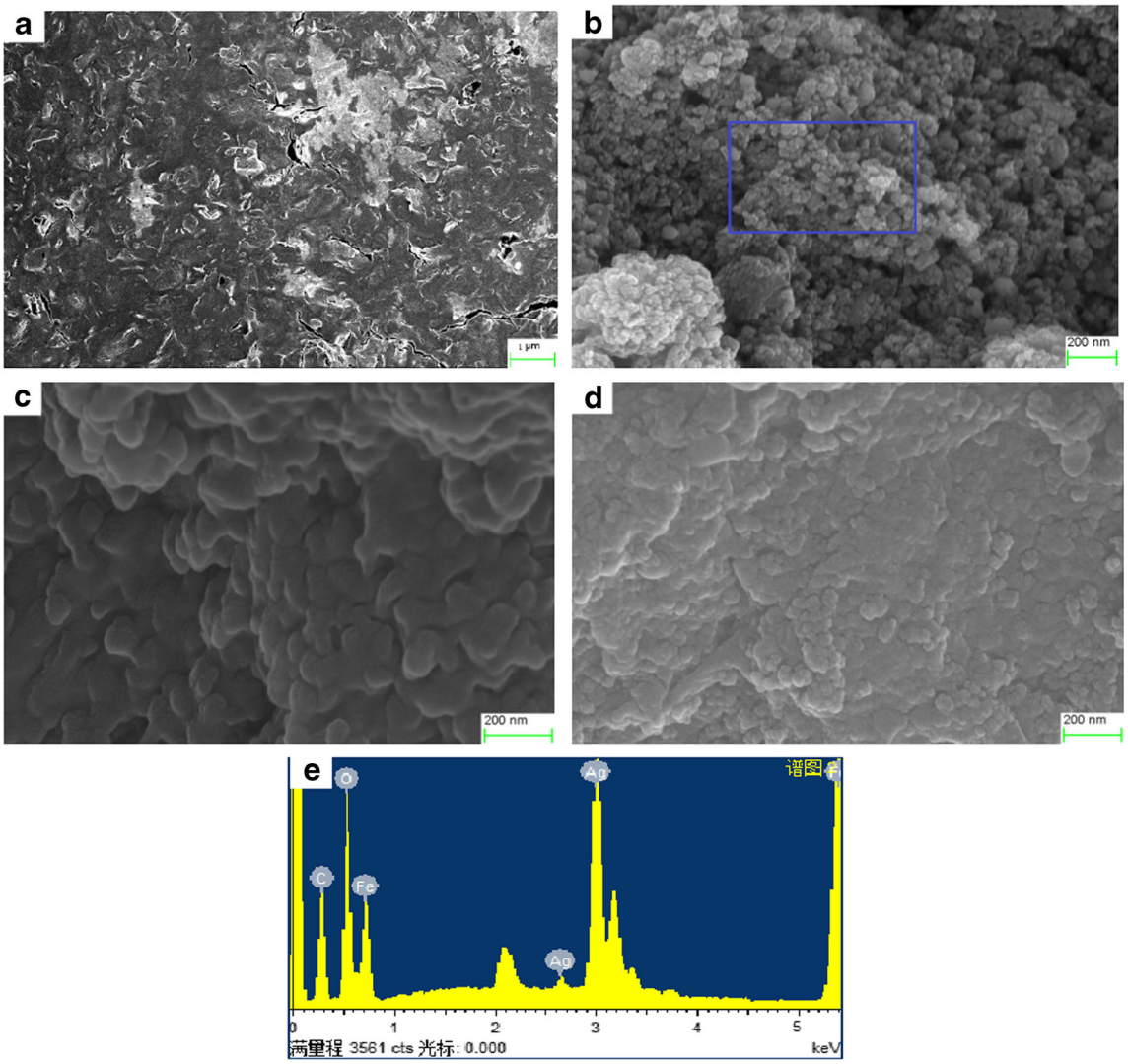

Fig. 2 FE-SEM images of SPE (**a**), SPE│MrGO (**b**), SPE│MrGO-MIP (**c**), SPE│MrGO-NIP (**d**) electrodes and EDS of marked area in SEM image of SPE│MrGO electrode (**e**)

the immobilized NIP hinders the electron exchanges without the excess of QR may accelerate the electron exchanges.

The electrochemical behaviors recorded on different electrodes in 0.1 M pH = 7.0 PB containing 1.0×10^2 μM QR are

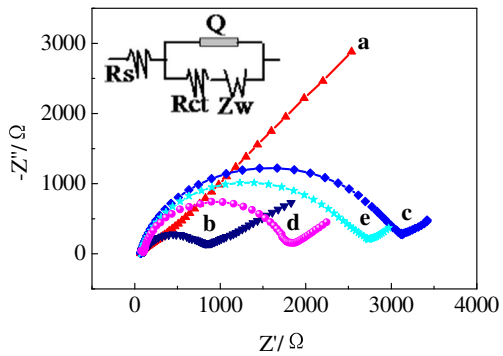

Fig. 3 EISs of 10 mmol·L^{-1} $[Fe(CN)_6]^{3-/4-}$ and 0.1 mol·L^{-1} KCl at SPE (**a**), SPE│MrGO (b), SPE│MrGO-MIP before (**c**) or after elution (**d**) and SPE│MrGO-NIP (**e**) electrodes

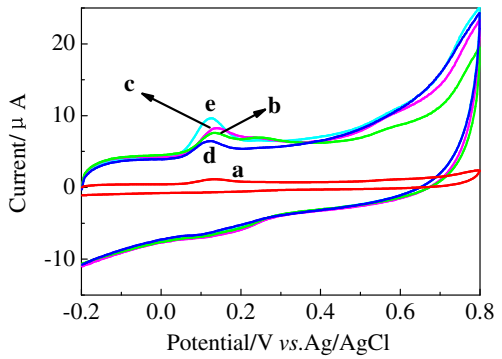

Fig. 4 CVs of SPE (**a**), SPE│MrGO (**b**), SPE│MrGO-MIP (**c**), SPE│MrGO-NIP (**d**) electrodes in presence of 1.0×10^2 μM QR and (**c**) electrode added with 1.5×10^2 μM QR (**e**). *v*: 0.1 V·s^{-1}

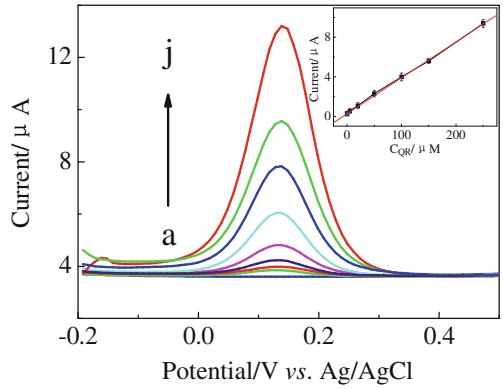

Fig. 5 DPVs of SPE| MrGO-MIP electrode in PB containing 0 (**a**), 0.02 (**b**), 0.2 (**c**), 5.0 (**d**), 20.0 (**e**), 50.0 (**f**), 100.0 (**g**), 150.0 (**h**), 250.0 (**i**) μM of QR. Insets: the calibration curves of ipa vs.C_{QR}

shown in Fig. 4. The redox peak currents increases remarkably on the SPE| MrGO electrode (Fig. 4b) compared with SPE electrode (Fig. 4a), indicating the reversibility of QR on the SPE| MrGO electrode increases. The result can be ascribed to the presence of conductive MrGO immobilized on the electrode, which provides porous structures for electrons exchanging of QR. The SPE| MrGO-MIP electrode (Fig. 4c) exhibits higher redox peak current than SPE| MrGO electrode. That indicates that MIP has stronger absorbability toward the QR. However, the response of SPE| MrGO-NIP (Fig. 4d) electrode is lower than SPE| MrGO electrode but still higher than SPE electrode. It may be that the electron block effect of NIP to current reduction is lower than the synergistic effect of MrGO to current amplification. Moreover, the redox peak current on the SPE| MrGO-MIP electrode increases with the increased QR concentration (Fig. 4e). The result reveals the potential application of SPE| MrGO-MIP electrode in QR analysis.

Optimization of method

The following parameters were optimized: (a) The volume of MrGO-MIP solution; (b) The accumulation time and accumulation potential; (c) Sample pH value. Respective data and Figures are given in the Electronic Supporting Material (ESM). We found the following experimental conditions to give the best results: (a) The volume of MrGO- MIP solution of 10.0 μL; (b) The accumulation time and accumulation potential of 600 s and +0.05 V (vs. Ag/AgCl); (c) Sample pH value of 7.0 (Fig. S4).

The detection of quercetin on the SPE|MrGO-MIP electrode

Under optimal experimental conditions, the DPVs of the SPE| MrGO-MIP electrode toward various concentrations of QR are shown in Fig. 5. Well-defined ipas are proportional to the concentrations of QR (C_{QR}) in the linear detection ranges (LDR) of 2.0×10^{-2} to 2.5×10^{2} μM. The linearization equation is: ipa(μA) = 0.3356 + 0.036C_{QR}(μM) (R = 0.9995). The limit of detection (LOD) is 1.3×10^{-2} μM (S/N = 3).

Compared with several QR electrochemical sensor reported previously (Tab. 1), the modified electrode presented with excellent comprehensive performances. The surface of modified electrode can be renewed quickly with external magnetic fields in terms of the advantages of Fe_3O_4 magnetic nanoparticle. It also shows a wide LDR and a low LOD. Those may be attributed to the synergistic effects resulted from the combination of those particles.

Stability, reproducibility and selectivity of the modified electrode

The modified electrode was stored at room temperature in drying conditions. The current response to 1.0×10^{2} μM QR kept about 91.1% of the initial value after six weeks, suggesting a long-range stability of the modified electrode.

The reproducibility of the modified electrode was first valued at a QR concentration of 1.0×10^{2} μM with the same SPE| MrGO-MIP electrode. For six successive assays, the relative standard deviation ($R.S.D.$) was 3.3%. Six SPE| MrGO -MIP electrodes fabricated independently were employed to determine 1.0×10^{2} μM of QR to check the

Table 1 Comparison of variouos electrochemical sensors for quercetin (data in μM)

Sensors	Renewable	LDR	LOD	Ref.
ASG[a]/CPE[b]	Slow	0.0165–0.3309	12	[1]
Pt-PDA@SiO_2/GCE	Slow	0.05–0.383	16	[10]
GQD[c]/AuNP[d]/GCE	Slow	0.01–6.0	0.002	[11]
Co_3O_4/GCE	Slow	0.50–330	100	[36, 37]
MIP/GO/GCE	Slow	0.6–15	48	[38]
TiO_2/PtP[e]/GCE	Slow	0.0059–148.0	0.0024	[39]
CTAB@Fe-MWCNTs[f]/CPE	Slow	0.06–3000	0.0012	[40]
SPE| MrGO-MIP	Quick	0.02–250.0	0.013	This work

[a] Activated silica gel, [b] Carbon paste electrode, [c] Graphene quantum dot, [d] Gold nanoparticle, [e] Pt(II)-porphyrin complex, [f] Iron decorated multi-walled carbon nanotubes

Table 2 Determination results of QR in medicinal tablets ($n = 5$, values are mean ± standard error)

Samples	Spiking/μM	Detected/μM	Added/μM	Found/μM	*R.S.D.*/%	Recovery/%
1	39.7	39.2 ± 0.032	50.0	91.35 ± 0.025	2.54	104.3
2	39.7	40.0 ± 0.045	50.0	91.25 ± 0.022	4.16	102.5
3	39.7	38.9 ± 0.021	50.0	90.50 ± 0.039	3.77	103.2
4	39.7	39.7 ± 0.033	50.0	89.45 ± 0.041	4.01	99.5

electrode-to-electrode reproducibility. An acceptable reproducibility with *R.S.D.* of 2.7% was obtained.

Several substances that may interfere the responses of the modified electrode were evaluated. A relative error less than ±5% is defined as the selectivity of the modified electrode for 10.0 μM QR determination. No interference was observed with addition of 200-fold concentrations of Na^+, K^+, Mg^{2+}, Ca^{2+}, Zn^{2+}, NO_3^- and SO_4^{2-}, 50-fold concentrations of fructose, lactose, glucose, sucrose and urea, 20-fold concentrations of UA, AA, dopamine, L-cysteine, glycine and phenol. The interference of other flavonoids such as rutin, hyperin, delphindin and cyaniding are also studied. 10-fold concentrations of hyperin, delphindin and cyaniding did not exert negative effects to QR. However, only a small amount of rutin (≤3 folds) is acceptable in the determination of QR due to their similar structure. The results demonstrate the good selectivity.

Application on medicinal tablets

The modified electrode was employed to determine QR in medicinal tablets to test the reliability of this method. One QR medicinal tablet (labeled amount: 1.20 mg) was grinded to a fine powder then extracted with 50 mL ethanol in the ultrasonic bath for 15 min. The solution was diluted into 100 mL with the supporting electrolyte after filtration. Five parallel determinations were performed and the results are shown in Table 2. The standard QR solution was added into solution and the recoveries were detected after each determination. The detected contents in the medicine tablets were in good accordance to the labeled value. The recoveries were evaluated between 99.5% and 104.3%. The results indicate that the present method possesses good precision and accuracy for determining of QR in real sample.

Conclusions

The highly sensitive and selective sensing platform based on disposable electrode for QR determination using MrGO-MIP composite modified SPE was fabricated. Attributing to the synergistic effect resulted from the combination of hybrid composite, the modified electrode shows the merits of wide LDR, low LOD, renewable as well as disposable design. By measuring the medicinal tablets, the practical application of QR electrochemical sensor is evaluated. It exploits new ways for magnetic MIP based composite in drug and food residues determination. Moreover, the universal sensing platform can be explored to determine other drugs and foods.

Acknowledgements The authors appreciate the support of the National Natural Science Foundation of China (Nos. 51672104 and 51472107), the Natural Science Foundation of Hunan Province (No. 2016JJ4071), the Foundation of Hunan Educational Committee (Nos. 16B205 and 17C1148), the Construct Program of the Key Discipline in Huaihua University and the Hunan Province Food & Drug Testing and Quality Control School-Enterprise Cooperation Innovation and Entrepreneurship Education Base.

Compliance with ethical standards The author(s) declare that they have no competing interests.

References

1. Chen XR, Li Q, Yu S, Lin B, Wu K (2012) Activated silica gel based carbon paste electrodes exhibit signal enhancement for quercetin. Electrochim Acta 81:106–111. https://doi.org/10.1016/ j.electacta.2012.07.063
2. Zhang Z, Miao Y, Lian L, Yan G (2015) Detection of quercetin based on Al^{3+}-amplified phosphorescence signals of manganese-doped ZnS quantum dots. Anal Biochem 489:17–24. https://doi.org/10.1016/j.ab.2015.08.002
3. Wang Y, Cao J, Weng JH, Zeng S (2005) Simultaneous determination of quercetin, kaempferol and isorhamnetin accumulated human beast cancer cells, by high-performance liquid chromatography. J Pharm Biomed Anal 39:328–333. https://doi.org/10.1016/j.jpba.2005.03.016
4. Qiu H, Luo C, Sun M, Lu F, Fan L, Li X (2012) A novel chemiluminescence sensor for determination of quercetin based on molecularly imprinted polymeric microspheres. Food Chem 134:469–473. https://doi.org/10.1016/j.foodchem.2012.02.102
5. Wang Q, Ding F, Li H, He P, Fang Y (2003) Determination of hydrochlorothiazide and rutin in Chinese herb medicines and human urine by capillary zone electrophoresis with amperometric detection. J Pharmaceut Biomed 30:1507–1514. https://doi.org/10.1016/S0731-7085 (02)00540-X
6. Nikolovska-Coleska Z, Klisarova LJ, Suturkova LJ, Dorevski K (1996) First and secondderivative spectrophotometric determination of flavonoids chrysin and quercetin. Anal Lett 29:97–115. https://doi.org/10.1080/00032719608000395

7. Zhang Z, Gu S, Ding Y, Shen M, Jiang L (2014) Mild and novel electrochemical preparation of β-cyclodextrin/graphene nanocomposite film for super-sensitive sensing of quercetin. Biosens Bioelectron 57:239–244. https://doi.org/10.1016/j.bios.2014.02.014
8. Lin XQ, He JB, Zha ZG (2006) Simultaneous determination of quercetin and rutin at a multi-wall carbon-nanotube paste electrodes by reversing differential pulse voltammetry. Sensors Actuators B Chem 119:608–614. https://doi.org/10.1016/j.snb.2006.01.016
9. Vilian Ezhil AT, Puthiaraj P, Kwak CH, Choe SR, Huh YS, Ahn WS, Han YK (2016) Electrochemical determination of quercetin based on porous aromatic frameworks supported au nanoparticles. Electrochim Acta 216:181–187. https://doi.org/10.1016/j.electacta.2016.08.150
10. Manokaran J, Muruganantham R, Muthukrishnaraj A, Balasubramanian N (2015) Platinum-polydopamine @SiO_2 nanocomposite modified electrode for the electrochemical determination of quercetin. Electrochim Acta 168:16–24. https://doi.org/10.1016/j.electacta.2015. 04.016
11. Li JJ, Qu JJ, Yang R, Qu LB, Harrington PDB (2016) A sensitive and selective electrochemical sensor based on graphene quantum dot/gold nanoparticle nanocomposite modified electrode for the determination of quercetin in biological samples. Electroanalysis 28:1–10. https://doi.org/10.1002/elan.20150049
12. Uzun L, Turner APF (2016) Molecularly-imprinted polymer sensors: realising their potential. Biosens Bioelectron 76:131–144. https://doi.org/10.1016/j.bios.2015.07.013
13. Yanez-Sedeno P, Pingarron JM (2017) Electrochemical sensors based on magnetic molecularly imprinted polymers: a review. Anal Chim Acta 960:1–17. https://doi.org/10.1016/j.aca. 2017.01.003
14. Salmi Z, Benmehdi H, Lamouri A, Decorse P, Jouini M, Yagci Y, Chehimi MM (2013) Preparation of MIP grafts for quercetin by tandem aryl diazonium surface chemistry and photopolymerization. Microchim Acta 180:1411–1419. https://doi.org/10.1007/s00604-013-0993-8
15. Yang L, Xu BJ, Ye HL, Zhao FQ, Zeng BZ (2017) A novel quercetin electrochemical sensor based on molecularly imprinted poly(para-aminobenzoic acid) on 3D Pd nanoparticles-porous graphene-carbon nanotubes composite. Sensors Actuators B Chem 251:601–608. https://doi.org/10.1016/j.snb.2017.04.006
16. Gholivand MB, Shamsipur M, Dehdashtian S, Rajabi HR (2014) Development of a selective and sensitive voltammetric sensor for propylparaben based on a nanosized molecularly imprinted polymer-carbon paste electrode. Mater Sci Eng C 36:102–107. https://doi.org/10.1016/j.msec.2013.11.021
17. Zhu WY, Jiang GY, Xu L, Li BZ, Cai QZ, Jiang HJ, Zhou XM (2015) Facile and controllable one-step fabrication of molecularly imprinted polymer membrane by magnetic field directed self-assembly for electrochemical sensing of glutathione. Anal Chim Acta 886:37–47. https://doi.org/10.1016/j.aca.2015.05.036
18. Liu P, Zhang XH, Xu W, Guo CH, Wang SF (2012) Electrochemical sensor for the determination of brucine in human serum based on molecularly imprinted poly-o-phenylenediamine/SWNTs composite film. Sensors Actuators B Chem 163:84–89. https://doi.org/10.1016/j.snb.2012.01.011
19. Zeng YB, Zhou Y, Zhou TS, Shi GY (2014) A novel composite of reduced graphene oxide and molecularly imprinted polymer for electrochemical sensing 4-nitrophenol. Electrochim Acta 130:504–511. https://doi.org/10.1016/j.electacta.2014.02.130
20. Li JH, Xu ZF, Liu MQ, Deng PH, Tang SP, Jiang JB, Feng HB, Qian D, He LZ (2017) Ag/N-doped reduced graphene oxide incorporated with molecularly imprinted polymer: an advanced electrochemical sensing platform for salbutamol determination. Biosens Bioelectron 90:210–216. https://doi.org/10.1016/j.bios.2016.11.016
21. Han Q, Wang X, Yang Z, Zhu W, Zhou X, Jiang H (2014) Fe_3O_4@rGO doped molecularly imprinted polymer membrane based on magnetic field directed self-assembly for the determination of Amaranth. Talanta 123:101–108. https://doi.org/10.1016/j.talanta.2014.01.060
22. Yang X, Ouyang YJ, Wu F, Hu YJ, Ji Y, Wu ZY (2017) Size controllable preparation of gold nanoparticles loading on graphene sheets@cerium oxide nanocomposites modified gold electrode for nonenzymatic hydrogen peroxide detection. Sensors Actuators B Chem 238:40–47. https://doi.org/10.1016/j.snb.2016.07.016
23. Liu GZ, Jiang W, Wang YP, Zhong ST, Sun DP, Liu J, Li FS (2015) One-pot synthesis of ag@Fe_3O_4/reduced graphene oxide composite with excellent electromagnetic absorption properties. Ceram Int l41:4982-4988. https://doi.org/10.1016/j.ceramint.2014.12.063
24. Song XL, Li JH, Wang JT, Chen LX (2009) Quercetin molecularly imprinted polymers: preparation, recognition characteristics and properties as sorbent for solid-phase extraction. Talanta (2):694–702. https://doi.org/10.1016/j.talanta.2009.07.051
25. Peng L, Wang YZ, Zeng H, Yuan Y (2011) Molecularly imprinted polymer for solid-phase extraction of rutin in complicated traditional Chinese medicines. Analyst 136:756–763. https://doi.org/10.1039/C0AN00798F
26. Xu J, Wang Y, Hu S (2017) Nanocomposites of graphene and graphene oxides: synthesis, molecular functionalization and application in electrochemical sensors and biosensors. A review. Microchim Acta 184:1–44. https://doi.org/10.1007/s00604-016-2007-0
27. Nasir M, Nawaz MH, Latif U, Yaqub M, Hayat A, Rahim A (2017) An overview on enzyme-mimicking nanomaterials for use in electrochemical and optical assays. Microchim Acta 184:323–342. https://doi.org/10.1007/s00604-016-2036-8
28. Veerapandian M, Seo YT, Yun K, Lee MH (2014) Graphene oxide functionalized with silver@ silica-polyethylene glycol hybrid nanoparticles for direct electrochemical detection of quercetin. Biosens Bioelectron 58:200–204. https://doi.org/10.1016/j.bios.2014.02.062
29. Erogul S, Bas SZ, Ozmen M, Yildiz S (2015) A new electrochemical sensor based on Fe_3O_4 functionalized graphene oxide-gold nanoparticle composite film for simultaneous determination of catechol and hydroquinone. Electrochim Acta 186:302–313. https://doi.org/10.1016/j.electacta.2015.10.174
30. Yao ZF, Yang X, Wu F, Wu WL, Wu FP (2016) Synthesis of differently sized silver nanoparticles on a screen-printed electrode sensitized with a nanocomposites consisting of reduced graphene oxide and cerium (IV) oxide for nonenzymatic sensing of hydrogen peroxide. Microchim Acta 183:2799–2806. https://doi.org/10.1007/s00604-016-1924-2
31. Yang X, Wu F, Chen DZ, Lin HW (2014) An electrochemical immunosensor for rapid determination of clenbuterol by using magnetic nanocomposites to modify screen printed carbon electrode based on competitive immunoassay mode. Sensors Actuators B Chem 192:529–535. https://doi.org/10.1016/j.snb.2013.11.011
32. Hu J, Dong YL, Chen XJ, Zhang HJ, Zheng JM, Wang Q, Chen XG (2014) A highly efficient catalyst: in situ growth of au nanoparticles on graphene oxide-Fe_3O_4 nanocomposite support. Chem Eng J 236:1–8. https://doi.org/10.1016/j.cej.2013.09.080
33. Xu HY, Shao MW, Chen T, Zhuo SJ, Wen CY, Peng MF (2012) Magnetism-assisted assembled porous Fe_3O_4 nanoparticles and their electrochemistry for dopamine sensing. Microporous Mesoporous Mater 153:35–40. https://doi.org/10.1016/j.micromeso.2011.12.032
34. Yang X, Xiao FB, Lin HW, Wu F, Chen DZ, Wu ZY (2013) A novel H_2O_2 biosensor based on Fe_3O_4-au magnetic nanoparticles coated horseradish peroxidase and graphene sheets-nafion film

modified screen-printed carbon electrode. Electrochim Acta 109: 750–755. https://doi.org/10.1016/j.electacta.2013.08.011

35. Zhang XY, Peng Y, Bai JL, Ning BA, Sun SM, Hong XD, Liu YY, Liu Y, Gao ZX (2014) A novel electrochemical sensor based on electropolymerized molecularly imprinted polymer and gold nanomaterials amplification for estradiol detection. Sensors Actuators B Chem 200:69–75. https://doi.org/10.1016/j.snb.2014.04.028
36. Abdel-Hamid R, Rabia MK, Newair EF (2016) Electrochemical behaviour of antioxidants: part 2. Electrochemical oxidation mechanism of quercetin at glassy carbon electrode modified with multiwall carbon nanotubes. Arab J Chem 9:350–356. https://doi.org/10.1016/ j.arabjc.2012.06.014
37. Wang M, Zhang D, Tong Z, Xu X, Yang X (2010) Voltammetric behavior and the determination of quercetin at a flowerlike Co_3O_4 nanoparticles modified glassy carbon electrode. J Appl Electrochem 41:189–196. https://doi.org/10.1007/s10800-010-0223-6
38. Sun S, Zhang M, Li Y, He X (2013) A molecularly imprinted polymer with incorporated graphene oxide for electrochemical determination of quercetin. Sensors 13:5493–5506. https://doi.org/10.3390/s130505493
39. Tian L, Wang B, Chen R, Gao Y, Chen Y, Li T (2015) Determination of quercetin using a photo-electrochemical sensor modified with titanium dioxide and a platinum (II)-porphyrin complex. Microchim Acta 182:687–693. https://doi.org/10.1007/s00604-014-1374-7
40. Erady V, Mascarenhas RJ, Satpati AK, Detriche S, Mekhalif Z, Delhalle J, Dhason A (2016) A novel and sensitive hexadecyltrimethylammoniumbromide functionalized Fe decorated MWCNTs modified carbon paste electrode for the selective determination of quercetin. Mater Sci Eng C 76:114–122. https://doi.org/10.1016/j.msec.2017.03.082